

# Parity breaking in Thouless quantum walks

Carlo Danieli,<sup>1</sup> Laura Pilozzi,<sup>1,2,\*</sup> Claudio Conti,<sup>3,2</sup> and Valentina Broscio<sup>1</sup>

<sup>1</sup>*Institute for Complex Systems, National Research Council (ISC-CNR), Via dei Taurini 19, 00185 Rome, Italy*

<sup>2</sup>*Research Center Enrico Fermi, Via Panisperna 89a, 00184 Rome, Italy*

<sup>3</sup>*Department of Physics, University of Sapienza, Piazzale Aldo Moro 5, 00185 Rome, Italy*

(Dated: December 4, 2024)

Non-Abelian evolution is a landmark in modern theoretical physics. But if non-commutative dynamics has a significant impact in the control of entanglement and transport in quantum systems is an open question. Here we propose to utilize non-Abelian Thouless pumping in one-dimensional discrete-time quantum walks in lattices with degenerate Bloch-bands. We show how the interplay of non-commutativity and topology enables geometrically protected quantum coin and shift operators. By composing different non-Abelian pumping cycles, different classes of tunable protected quantum walks arise. Surprisingly, the walks break parity symmetry and generate a dynamic process described by a Weyl-like equation. The amount of entanglement can be varied by acting on the initial conditions. The asymptotic statistical distribution and its features are determined by closed form analytical expression and confirmed numerically.

Quantum walks [1–7], introduced as the quantum counterpart to classical random walks, utilize quantum interference to extend the walker’s path length and shape the final statistical distribution. Their computational universality [2] makes them a powerful tool for developing more efficient quantum algorithms [3, 4], offering quantum speedup [8–11] in tasks like quantum search [12, 13] and simulation [14].

Beyond quantum computing, quantum walks have been used to study topological phenomena [15–19], Anderson localization [20, 21], and investigate both classical [22–24] and quantum [25–29] correlations. They have been implemented on various platforms [30–32], like superconducting qubits [18, 33], nuclear magnetic resonance [34], and optical systems [35, 36].

Quantum walks take place on graphs  $\mathcal{G} = (\mathcal{V}, \mathcal{E})$ , where the vertices  $\mathcal{V}$  represent the sites the walker can visit, and the edges  $\mathcal{E}$  define the connections between the sites. While space in quantum walks is discrete [4], time can be either discrete or continuous – yielding continuous-time [2, 3] and discrete-time [5, 6] quantum walks. The state of the walker is described by its position on the graph and a quantum coin variable, such as spin. In the discrete-time case, the walker evolves through a sequence of unitary maps, each consisting of a coin operator  $\mathcal{R}$ , which acts on the coin state, and a conditional shift operator  $\mathcal{T}$ , which moves the walker depending on the coin state. The Hadamard’s is a common quantum coin operator [7], however, quantum walks can be defined with different parametric families of quantum coin operators for better control and optimization [37, 38].

In this work, we show that discrete-time quantum walks (DTQWs) can be naturally implemented utilizing non-Abelian Thouless pumping [39–41]. Thouless pumping is a paradigmatic topological phenomenon yielding quantized transport in slowly and cyclically modulated one-dimensional lattices [42]. In systems with degenerate Bloch bands Thouless pumping acquires a non-Abelian

character [39]. In this case, the system is initially prepared in a Wannier state belonging to a degenerate band and undergoes a geometric evolution dictated by the Wilczek–Zee connection [43].

Here, we utilize non-Abelian Thouless pumping to generate DTQWs in a Lieb chain with two degenerate flat bands [44–47]. Specifically, we construct two pumping cycles acting as coin and shift operators on localized state. Remarkably, these cycles are protected against dynamical perturbations [39] and enable the implementation of arbitrary unitary coins—beyond the standard Hadamard coin—and unidirectional conditional shifts.

We call this new family of one-dimensional quantum walks *Thouless holonomic quantum walks* (ThQWs). The structure of ThQWs is intimately related to the topological character of the two degenerate bands and it can be engineered by suitably defining the elementary pumping cycles.

We show that Thouless quantum walks offer a high level of flexibility and enable to selectively break parity or time-reversal symmetry allowing to engineer different final quantum correlated states. By estimating analytically the asymptotic distribution of the walker, we fully characterize these correlations and the dynamic process generated by ThQWs depending on the initial conditions and the coin operator. In particular, the entanglement between position and coin is explicitly calculated. The parity-broken nature of Thouless quantum walks is further illustrated by relating the dynamic equation describing the walk to the Weyl equation. We focus on the implementation in photonic waveguides [39, 48] where the role of time is played by the coordinate along the waveguide, denoted as  $z$  as shown in Fig. 1(e-f), but our results can be extended to cold atoms in optical lattices [49] and superconducting nanocircuits [50].

In the simplest model of discrete time quantum walks, the walker moves along a line and has two coin levels,  $\pm$ . In this case, the shift and coin operators can be written

as:

$$\mathcal{T} = \sum_n \left[ |n + \delta_+\rangle \langle n| \otimes |+\rangle \langle +| + |-\rangle \langle -| \otimes |n + \delta_-\rangle \langle n| \right]$$

$$\mathcal{R} = \sum_n |n\rangle \langle n| \otimes \begin{pmatrix} \cos \theta & \sin \theta \\ -\sin \theta & \cos \theta \end{pmatrix}.$$

where the integers  $\delta_\sigma$  denote the shifts of the states  $|n, \sigma\rangle = |n\rangle \otimes |\sigma\rangle$ .

Implementing  $\mathcal{T}$  and  $\mathcal{R}$  by means of non-Abelian Thouless pumping requires introducing two orthogonal states,  $|p_n\rangle$  and  $|q_n\rangle$ , playing the role of coin states, and designing two pumping cycles,  $\mathcal{C}_\mathcal{T}$  and  $\mathcal{C}_\mathcal{R}$ , of period  $\lambda_\mathcal{T}$  and  $\lambda_\mathcal{R}$ , yielding conditional shift and coin operators. The composition  $\mathcal{C} = \mathcal{C}_\mathcal{T} \circ \mathcal{C}_\mathcal{R}$  yields one quantum walk step of duration  $\lambda = \lambda_\mathcal{T} + \lambda_\mathcal{R}$ .

The discrete nature of the resulting ThQW is enforced by the topology of the lattice and the geometric structure of the cycle. This naturally generates a quantized motion made of steps connecting one unit cell to the next where each step takes one pumping period. The pumping period,  $\lambda$ , therefore represents the time unit of the quantum walk. The state of the walker after  $t$  steps with  $t \in \mathbb{Z}$  is described by the wavefunction  $|\Psi(z_t)\rangle$  with  $z_t = z_0 + \lambda t$  and  $|\Psi(z_{t+1})\rangle = \mathcal{C}|\Psi(z_t)\rangle$ .

We now consider the implementation of ThQW in a chain with two degenerate flat bands [39], reminiscent of the two-dimensional Lieb lattice [51]. The Hamiltonian features four sites *per* unit cell indicated respectively as *a, b, c* and *d* and it reads

$$H = \sum_n \left( J_{b1} a_n^\dagger b_n + J_{b2} a_n^\dagger b_{n-1} + J_c a_n^\dagger c_n + J_d a_n^\dagger d_n + \text{H.c.} \right) \quad (1)$$

where  $x_n^\dagger$  and  $x_n$  denote the creation and the annihilation operators on sites  $x = a, b, c, d$  of the cell  $n$ . For any choice of the hopping parameters, the spectrum consists of two non-dispersive modes with longitudinal momentum  $\kappa_0 = 0$  and two dispersive modes with longitudinal momenta  $\kappa_\pm(k) = \pm\Delta(k)$  with  $\Delta(k) = \sqrt{J_c^2 + J_d^2 + |J_b(k)|^2}$  and  $J_b = J_{b1} + J_{b2}e^{ik}$ . The chiral symmetry of the lattice [52] implies that the Bloch states corresponding to  $\kappa_0$  can be written as

$$|\phi_1\rangle = \frac{J_c|d_k\rangle - J_d|c_k\rangle}{\delta}$$

$$|\phi_2\rangle = \frac{-\delta^2|b_k\rangle + J_b^*(J_c|c_k\rangle + J_d|d_k\rangle)}{\delta\Delta(k)} \quad (2)$$

with  $\delta = \sqrt{J_c^2 + J_d^2}$ . An adiabatic pumping cycle  $\mathcal{C}$  acting on the system initially prepared in a Wannier state,  $|\Psi(z_0)\rangle$ , belonging to the non-dispersive modes then yields [53]

$$|\Psi(z_1)\rangle = \sum_{k\ell m} \alpha_\ell [W_\mathcal{C}(z_1, z_0)]_{m\ell} |\phi_m(k, z_0)\rangle e^{ikn}$$

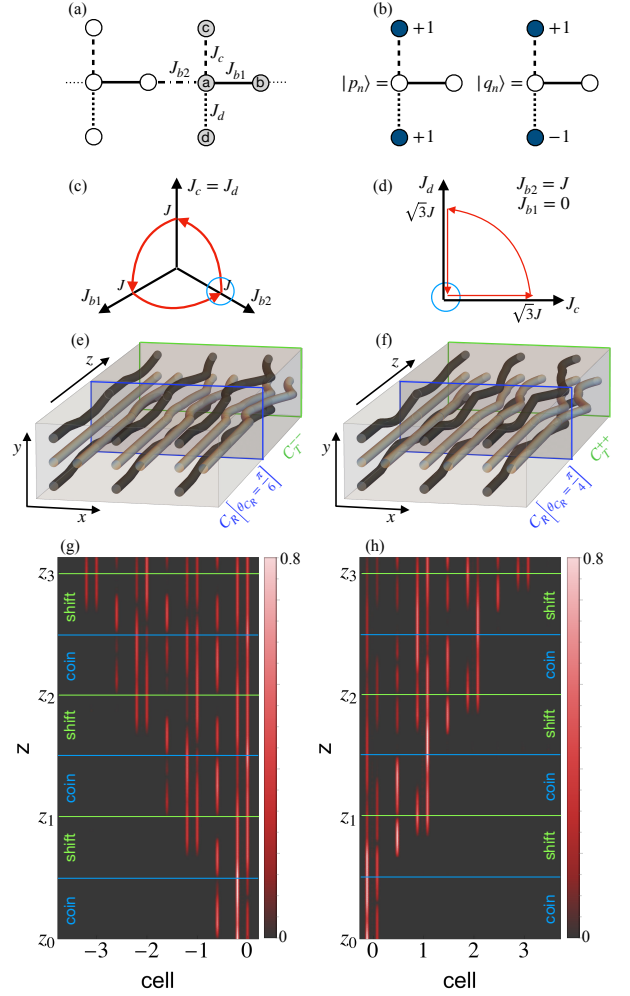


FIG. 1. (a) Lattice profile with the unit-cell coloured in grey. (b) Orthogonal symmetric  $|p_n\rangle$  and antisymmetric  $|q_n\rangle$  states with non-zero amplitudes coloured in dark blue. (c,d) Pumping cycles  $\mathcal{C}_\mathcal{T}^{++}$  and  $\mathcal{C}_\mathcal{R}$  respectively in the parameter space. The blue circles indicate the initial point. (e) Illustration of three unit-cells of the lattice pumped by cycle  $\mathcal{C}_\mathcal{R}$  with  $\theta_{\mathcal{C}_\mathcal{R}} = \pi/6$  (blue) and cycle  $\mathcal{C}_\mathcal{T}^-$  (green). (f) Same as (e) with  $\theta_{\mathcal{C}_\mathcal{R}} = \pi/4$  in cycle  $\mathcal{C}_\mathcal{R}$  and cycle  $\mathcal{C}_\mathcal{T}^{++}$ . (g) Three steps propagation of the walk from a single-cell excitation. The green lines indicate the time-units  $z_t$ , while the blue ones separate the coin  $\mathcal{C}_\mathcal{R}$  with  $\theta_{\mathcal{C}_\mathcal{R}} = \pi/6$  and shift  $\mathcal{C}_\mathcal{T}^-$ . (h) Same as (g) with  $\theta_{\mathcal{C}_\mathcal{R}} = \pi/4$  and cycle  $\mathcal{C}_\mathcal{T}^{++}$ .

where the coefficients  $\alpha_\ell$  define the initial Wannier state while  $W_\mathcal{C}(z_1, z_0)$ ,

$$W_\mathcal{C}(z_1, z_0) = \mathcal{P} \exp \left[ i \int_{z_0}^{z_1} \Gamma_0^z dz \right], \quad (3)$$

indicate the holonomy transformation associated with the Wilczek-Zee connection  $[\Gamma_z]_{\ell m} = \langle \phi_\ell(k, z) | i\partial_z | \phi_m(k, z) \rangle$  [39].

To engineer the ThQW we initialize the lattice setting  $J_c = J_d = J_{b1} = 0$  and  $J_{b2} = J$ . The Wannier states belonging to the non-dispersive modes defined by Eqs. (2)

can be then cast as

$$|q_n\rangle = \frac{|c_n\rangle - |d_n\rangle}{\sqrt{2}} \quad |p_n\rangle = \frac{|c_n\rangle + |d_n\rangle}{\sqrt{2}} \quad (4)$$

These states act as the two coin levels. Following Ref. [39], as discussed in more detail in [53], the pumping cycles implementing conditional shift and coin operators on these states can be straightforwardly designed. As shown in Fig. 1(c), the conditional shift operator cycles, denoted as  $\mathcal{C}_{\mathcal{T}}^{\xi s}$ , are represented by spherical triangles on the hyperplane  $J_c = sJ_d$  with  $s = \pm$ , having anti-clockwise ( $\xi = +1$ ) or clockwise ( $\xi = -1$ ) orientation. On the contrary, the coin operator cycle  $\mathcal{C}_{\mathcal{R}}$ , shown in Fig.1(d), lies on the plane  $\{J_{b2} = J, J_{b1} = 0\}$ . The corresponding holonomic transformations in  $k$ -space can be written as [39, 53]

$$W_{\mathcal{C}_{\mathcal{T}}^{\xi s}} = e^{i\xi\frac{k}{2}(\sigma_0 - s\sigma_z)} \quad W_{\mathcal{C}_{\mathcal{R}}} = e^{i\theta_{\mathcal{C}_{\mathcal{R}}}(\sin k\sigma_x + \cos k\sigma_y)} \quad (5)$$

with  $\sigma_i$  and  $\sigma_0$  denoting the Pauli matrices and the identity. From the above discussion it emerges that Thouless quantum walks have two crucial characteristics: (i) they yield conditional shifts determined by the topology of the driven bands; (ii) they offer the possibility to control the shift's direction by controlling the orientation of the pumping cycles, related to the index  $\xi$ . Moreover, in the specific example discussed here, they allow to select which of the two coin states,  $|p_n\rangle$  or  $|q_n\rangle$ , moves by changing the relative phase of  $J_c$  and  $J_d$ . Specifically, they implement the following operators:

$$\mathcal{C}_{\mathcal{T}}^{\xi+} : \sum_n \left[ |p_{n+\xi}\rangle\langle p_n| + |q_n\rangle\langle q_n| \right] \quad (6)$$

$$\mathcal{C}_{\mathcal{T}}^{\xi-} : \sum_n \left[ |p_n\rangle\langle p_n| + |q_{n+\xi}\rangle\langle q_n| \right] \quad (7)$$

thus resulting in right- and left- oriented uni-directional shift operators, respectively. Note that  $\mathcal{C}_{\mathcal{T}}^{\xi s}$  requires  $J_c = sJ_d$ . On the other hand, the cycle  $\mathcal{C}_{\mathcal{R}}$  yields zero displacement but it performs a rotation by an angle  $\theta_{\mathcal{C}_{\mathcal{R}}}$  which depends on its precise shape [39]. For example, the cycle shown in Fig. 1(d) corresponds to  $\theta_{\mathcal{C}_{\mathcal{R}}} = \frac{\pi}{4}$ . In this case, reversing the orientation of the pumping cycles inverts the rotation. Composing the cycles  $\mathcal{C}_{\mathcal{T}}^{\xi s}$  and the cycle  $\mathcal{C}_{\mathcal{R}}$  enables the realization of directional ThQWs with chirality  $\chi = \xi s$ , therefore breaking parity symmetry.

To illustrate this point, in Figures 1(e-h) we show two examples of ThQWs corresponding, respectively, to  $\mathcal{C} = \mathcal{C}_{\mathcal{T}}^- \mathcal{C}_{\mathcal{R}}$  with  $\theta_{\mathcal{C}_{\mathcal{R}}} = \pi/6$  (Fig. 1(e,g)) and  $\mathcal{C} = \mathcal{C}_{\mathcal{T}}^+ \mathcal{C}_{\mathcal{R}}$  with  $\theta_{\mathcal{C}_{\mathcal{R}}} = \pi/4$  (Fig. 1(f,h)). In Figures 1(g,h), we display the field intensity along the waveguides for a single unit-cell initial condition of the form  $|\Psi(z_0)\rangle = \frac{1}{\sqrt{5}}|p_0\rangle + \frac{2}{\sqrt{5}}|q_0\rangle$ . As one can see, ThQWs enable a remarkable control on field's propagation.

Characterizing the final state of the QW in the asymptotic limit of a large number of steps is of crucial relevance for the design of quantum algorithms [54–56].

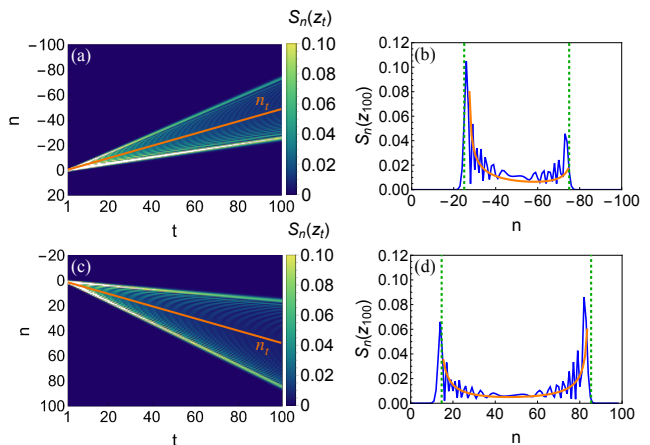


FIG. 2. (a) Left-oriented propagation of  $S_n$  for  $(a_0, b_0, \theta) = (\frac{1}{\sqrt{5}}, \frac{2}{\sqrt{5}}, \frac{\pi}{3})$ . (b) Distribution  $S_n(z_{100})$  numerically computed (blue) and analytically approximated (orange). The green dashed lines mark the boundaries of the distributions. (c,d) Same as (a,b) with right-oriented propagation and  $\theta = \frac{\pi}{4}$ .

To this end, we write the system wave-function after  $t$  steps as  $|\Psi(z_t)\rangle = \sum_n (\psi_n^p(z_t)|p_n\rangle + \psi_n^q(z_t)|q_n\rangle)$  and we express the corresponding probability distribution,  $S_n(z_t) = |\psi_n^p(z_t)|^2 + |\psi_n^q(z_t)|^2$ . Following Refs. [5, 6], at large  $z = z_t$  for arbitrary angles  $\theta$  and generic single unit cell initial conditions,  $|\Psi(z_0)\rangle = \sum_n \delta_{n,0}(a_0|p_n\rangle + b_0|q_n\rangle)$ , a wide range of properties can be estimated analytically [53].

The distribution  $S_n(z_t)$  is non-zero for  $\frac{-t \cos \theta}{2} < n - n_t < \frac{t \cos \theta}{2}$  while it drops exponentially outside this range [53]. The middle point  $n_t$  can be related to the first Chern number,  $C_1$ , that determines the average displacement of the states  $|p_n\rangle$  and  $|q_n\rangle$ . Specifically, we have  $n_t = \frac{C_1 t}{2}$ . Consistently, in the cycles  $\mathcal{C}_{\mathcal{T}}^{\xi s} \mathcal{C}_{\mathcal{R}}$  the Chern number is  $C_1 = \xi$  [39]. The shape of the distribution within the above window depends, not only on  $\theta$  but also on the initial conditions. For example, for  $\theta = 0$ , the final distribution simply consists of two peaks located respectively at the two extrema:  $n = 2n_t$  and  $n = 0$  whose weights are proportional to  $a_0$  and  $b_0$ . For arbitrary values of  $\theta$  the distribution has a more complex shape with fast oscillations superimposed to a bimodal envelope function, which can be approximated analytically as discussed in [53]. In Fig. 2(a-d) we exemplify the evolution and the final asymptotic state for a left and a right-oriented quantum walk. The comparison between the numerically computed asymptotic distributions (blue) and the analytically approximated envelope functions (orange), obtained by dropping the fast oscillating terms [53], is shown in Fig. 2(b,d), displays excellent agreement. The extrema of the interval are marked with vertical green dashed lines.

To illustrate the parity-broken nature of ThQWs it is useful to analyze the dynamic structure of the quantum

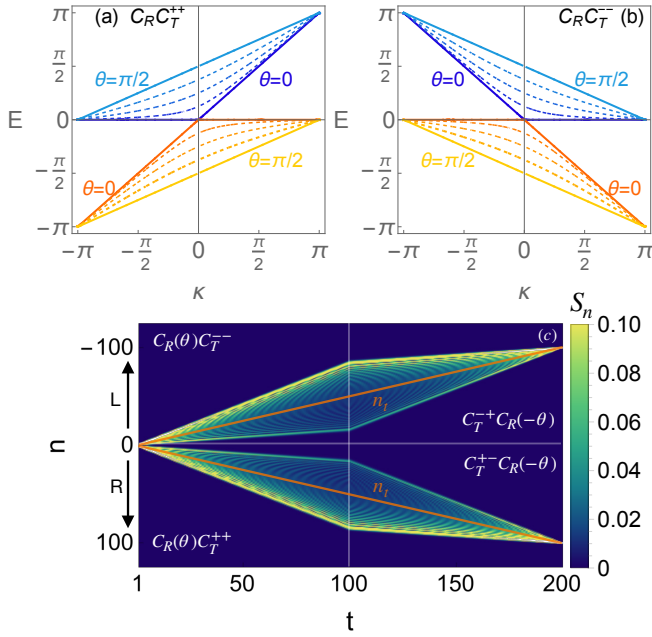


FIG. 3. Floquet quasi-energies for the quantum walks  $C_{\mathcal{R}}C_{\mathcal{T}}^{++}$  (a) and  $C_{\mathcal{R}}C_{\mathcal{T}}^{--}$  (b) for different values of the coin angle  $\theta \in [0, \pi/2]$  (c) Example of propagation along composite cycles. The pattern is generated by means of a two stage procedure. In the first stage we perform the  $C_{\mathcal{R}}C_{\mathcal{T}}^{++}$  for  $n \geq 0$  and  $C_{\mathcal{R}}C_{\mathcal{T}}^{--}$  for  $n \leq 0$  and suitably overlapping the two cycles for  $n = 0$ . In the second stage which starts at  $t = 100\lambda$ , we apply time-reversal symmetry and we exchange  $|p_n\rangle$  and  $|q_n\rangle$  while keeping the chirality  $\chi$  of the walks.

walk equations which following Ref. [57] can be written as

$$\partial_t \Psi = -\xi \left[ \cos \theta \frac{\sigma_0 + s\sigma_z}{2} + \sin \theta \frac{i\sigma_y + s\sigma_x}{2} \right] \partial_n \Psi + \quad (8)$$

$$+ [(\cos \theta - 1)\mathbb{I} + i \sin \theta \sigma_y] \Psi$$

with  $\Psi = (\psi_n^p(t), \psi_n^q(t))^T$  – see [53] for details. For  $\xi = +1$  and  $\xi = -1$  the above equation account for a right-moving or left-moving quantum walk as those shown in Fig. 2(a,c). In the limit  $\theta = 0$ , for each value of  $\xi$ , equation (8) describes a right-handed ( $\chi = +1$ ) and a left-handed ( $\chi = -1$ ) Weyl particle. Equivalently, the two Floquet quasi-energies  $E$  [53, 58] associated with the processes  $C_{\mathcal{R}}C_{\mathcal{T}}^{++}$  and  $C_{\mathcal{R}}C_{\mathcal{T}}^{--}$  produce two anisotropic bands whose structure depends on the angle  $\theta$ , as shown in Fig. 3(a) and Fig. 3(b). For  $\theta = 0$ , the system exhibits a flat band  $E = 0$  and a linearly dispersive band  $E = \xi k$  respectively associated to  $|q_n\rangle$  and  $|p_n\rangle$  in the cycle  $C_{\mathcal{R}}C_{\mathcal{T}}^{++}$  and the opposite for the cycle  $C_{\mathcal{R}}C_{\mathcal{T}}^{--}$ . For  $\theta \neq 0$ , the states  $|p_n\rangle$  and  $|q_n\rangle$  become coupled, yet the left-right directionality is preserved. Linear band dispersion  $E = \frac{\xi}{2}(k \pm \pi)$  is restored for  $\theta = \pi/2$  and the two states move in unison with half the group velocity of a single state with  $\theta = 0$  [53].

By composing quantum walks with different pari-

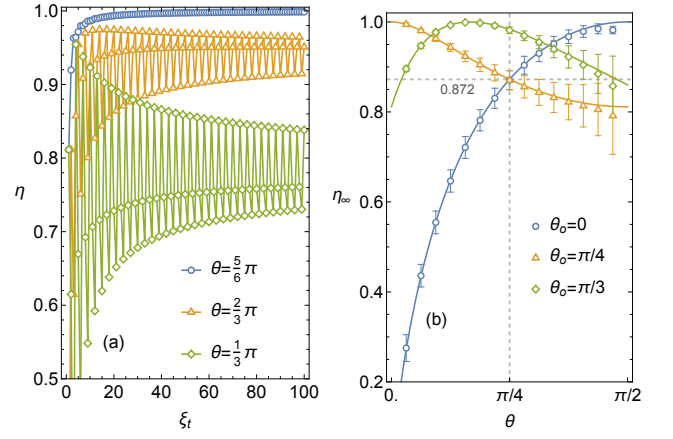


FIG. 4. (a) Dynamical evolution of the entropy  $\eta$  for  $\theta_0 = \frac{2\pi}{3}$  with  $\theta = \frac{5\pi}{6}$  (blue circles),  $\theta = \frac{\pi}{3}$  (orange triangles) and  $\theta = \frac{\pi}{3}$  (green diamonds). (b) Asymptotic entropy  $\eta_\infty$  of the entanglement as a function of  $\theta$  for different initial conditions. (c)  $\eta_\infty$  as function of  $\theta$  and  $\theta_0$ . The red dashed lines indicate where  $\eta_\infty = 1$ .

ties, more complex patterns can be generated. For instance, the pattern shown in Fig. 3(c) is produced through a two-stage procedure in which the quantum walks are combined with their counterparts obtained via the time-reversal operator and a chirality-preserving spin-inversion operator. In the first stage, the cycles  $C_{\mathcal{R}}C_{\mathcal{T}}^{++}$  (for  $n \geq 0$ ) and  $C_{\mathcal{R}}C_{\mathcal{T}}^{--}$  (for  $n \leq 0$ ) are performed, with an appropriate overlap at  $n = 0$  to ensure smooth connectivity. In the second stage, which begins after 100 steps, time-reversal symmetry is applied, and the roles of  $|p_n\rangle$  and  $|q_n\rangle$  are exchanged while keeping the chirality  $\chi$  of the time-reversed walks. This therefore involves combining quantum walks generated by the cycles  $C_{\mathcal{R}}(\theta)C_{\mathcal{T}}^{++}$  and  $C_{\mathcal{R}}(\theta)C_{\mathcal{T}}^{--}$  with those generated by  $C_{\mathcal{T}}^+C_{\mathcal{R}}(-\theta)$  and  $C_{\mathcal{T}}^-C_{\mathcal{R}}(-\theta)$ , respectively. The whole process maps the initial state  $(|p_0\rangle + |q_0\rangle)/\sqrt{2}$  onto the state  $(|q_{-t/2}\rangle + |p_{t/2}\rangle)/\sqrt{2}$  therefore generating quantum correlations between spin and position coordinates. This can be extended by considering more involved compositions of conditional shift cycles  $C_{\mathcal{T}}^{\xi s}$  and coin cycles  $C_{\mathcal{R}}$ , generalizing the class of ThQW achievable in photonic lattices. Moreover, varying periodically  $\theta$  in the cycle  $C_{\mathcal{R}}$  at every step  $z_t$  yields Floquet quantum walks [59], while varying  $\theta$  with  $n$  spatially modulates ThQWs, yielding topologically non trivial states – *e.g.* designing a splitstep advancement operator  $\mathcal{C} \equiv C_{\mathcal{T}}^- C_{\mathcal{R}}(\theta(n)) C_{\mathcal{T}}^{++} C_{\mathcal{R}}(\theta(n))$  as discussed in Ref. [60].

The quantum walk described by the distribution  $S_n(z_t)$  generates different kinds of quantum correlations. Here we focus on the entanglement [61] between coin state and position which can be quantified utilizing the von Neumann entropy,  $\eta = -\text{Tr}_\sigma[\rho_\sigma \ln \rho_\sigma]$ , where  $\rho_\sigma$  denotes the reduced density matrix obtained by tracing over the position index,  $\rho_\sigma = \text{Tr}_n[\rho]$  [62–64]. In

Fig. 4(a) we show the evolution of  $\eta$  for three angles  $\theta = \frac{5}{6}\pi, \frac{2}{3}\pi, \frac{1}{3}\pi$  starting from a single unit-cell excitation with  $(a_0, b_0) = (\cos\theta_0, \sin\theta_0)$  and  $\theta_0 = \frac{2}{3}\pi$ . As the number of steps grows,  $\eta$  oscillates and approaches the asymptotic value  $\eta_\infty$  that we calculate analytically from the eigenvalues of the asymptotic density matrix,  $\mu_{1,2} = \frac{1}{2} \left[ 1 \pm \frac{\cos(\theta - 2\theta_0)}{1 + \sin\theta} \right]$  [53].

In Fig. 4(b) we plot with solid lines the analytical results for  $\eta_\infty$  as a function of the coin angle  $\theta$  for different choices of  $\theta_0$  and compare them with numerical outcomes showing excellent agreement. Additionally, for  $\theta_0 = 0$  and the Hadamard coin  $\theta = \pi/4$ , the analytical results recover the asymptotic value  $\eta_\infty \approx 0.872$  obtained in Ref. [62] as shown in Fig. 4(b) with dashed lines. The expression of the eigenvalues  $\mu_1$  and  $\mu_2$  given above demonstrates that ThQWs achieve maximal entanglement,  $\eta_\infty = 1$ , for  $\theta = 2\theta_0 \pm \frac{\pi}{2}$  with  $\theta_0 \neq 0, \pi/2$ . Note that  $\eta_\infty = 1$  is fulfilled after a single step for  $\theta_0 = \pi/4$  while, close to  $\theta_0 = 0$  or  $\theta_0 = \pi/2$ , reaching  $\eta_\infty = 1$  requires an infinitely large number of steps [53].

In conclusion, exploiting non-Abelian dynamics is a frontier of quantum simulation and computing. In this Letter, we demonstrate that non-Abelian Thouless pumping allows to construct one-dimensional discrete-time quantum walks and exploiting symmetry breaking for a variety of applications. Quantum walks simulate diverse topological phases [15, 19]. The Lieb lattice discussed here highlights how the quantum walk directionality is tailored by the orientation of the pumping cycles. The topology of the bands in the Thouless pumping process breaks the natural parity-symmetry of the quantum walk, and affects the entanglement entropy remarkably.

In holonomic quantum computing [65–67], the computational space typically consists of a single localized quantum system. The present work shows that non-Abelian Thouless pumping allows to construct holonomic gates exploiting the lattice position to encode information and entangle it with local degrees of freedom. This circumstance opens novel strategies for quantum search algorithms based on holonomies.

Our analytical model describes in closed-form the pattern generated in the quantum walks and identifies the conditions for maximally entangled topologically protected states. The work can be extended in several directions, e.g. considering higher dimensional lattices with a more complex topological structure or widening the coin space.

#### ACKNOWLEDGMENT

The Authors acknowledge fruitful discussions with A. Coppo and A. Petri. This work was co-funded by European Union - PON Ricerca e Innovazione 2014-2020 FESR /FSC - Project ARS01.00734 QUANCOM,

Project PNRR MUR PE\_0000023-NQSTI and PNRR MUR project CN 00000013-ICSC.

\* [laura.pilozzi@cnr.it](mailto:laura.pilozzi@cnr.it)

- [1] Y. Aharonov, L. Davidovich, and N. Zagury, Quantum random walks, *Phys. Rev. A* **48**, 1687 (1993).
- [2] A. M. Childs, Universal computation by quantum walk, *Phys. Rev. Lett.* **102**, 180501 (2009).
- [3] E. Farhi and S. Gutmann, Quantum computation and decision trees, *Phys. Rev. A* **58**, 915 (1998).
- [4] J. Kempe, Quantum random walks: An introductory overview, *Contemporary Physics* **44**, 307 (2003).
- [5] A. Nayak and A. Vishwanath, Quantum walk on the line, *arXiv preprint quant-ph/0010117* (2000).
- [6] A. Ambainis, E. Bach, A. Nayak, A. Vishwanath, and J. Watrous, One-dimensional quantum walks, *STOC '01*, 37–49 (2001).
- [7] D. Aharonov, A. Ambainis, J. Kempe, and U. Vazirani, Quantum walks on graphs (2002), *arXiv:quant-ph/0012090* [quant-ph].
- [8] M. Szegedy, Spectra of quantized walks and a  $\sqrt{\delta\epsilon}$  rule (2004), *arXiv:quant-ph/0401053* [quant-ph].
- [9] L. K. Grover, A fast quantum mechanical algorithm for database search, in *Symposium on the Theory of Computing* (1996).
- [10] G. Brassard, P. Hoyer, M. Mosca, and A. Tapp, Quantum amplitude amplification and estimation, in *Quantum Computation and Information* (2002) pp. 53–74.
- [11] X. Qiang, S. Ma, and H. Song, Review on quantum walk computing: Theory, implementation, and application (2024), *arXiv:2404.04178* [quant-ph].
- [12] N. Shenvi, J. Kempe, and K. B. Whaley, Quantum random-walk search algorithm, *Phys. Rev. A* **67**, 052307 (2003).
- [13] S. D. Berry and J. B. Wang, Quantum-walk-based search and centrality, *Phys. Rev. A* **82**, 042333 (2010).
- [14] L. Sansoni, F. Sciarrino, G. Vallone, P. Mataloni, A. Crespi, R. Ramponi, and R. Osellame, Two-particle bosonic-fermionic quantum walk via integrated photonics, *Phys. Rev. Lett.* **108**, 010502 (2012).
- [15] T. Kitagawa, Topological phenomena in quantum walks: elementary introduction to the physics of topological phases, *Quantum Information Processing* **11**, 1107 (2012).
- [16] K. Mochizuki, T. Bessho, M. Sato, and H. Obuse, Topological quantum walk with discrete time-glide symmetry, *Phys. Rev. B* **102**, 035418 (2020).
- [17] A. Grudka, M. Karczewski, P. Kurzyński, J. Wójcik, and A. Wójcik, Topological invariants in quantum walks, *Phys. Rev. A* **107**, 032201 (2023).
- [18] E. Flurin, V. V. Ramasesh, S. Hacoheh-Gourgy, L. S. Martin, N. Y. Yao, and I. Siddiqi, Observing topological invariants using quantum walks in superconducting circuits, *Phys. Rev. X* **7**, 031023 (2017).
- [19] J. K. Asbóth, Symmetries, topological phases, and bound states in the one-dimensional quantum walk, *Phys. Rev. B* **86**, 195414 (2012).
- [20] I. Vakulchyk, M. V. Fistul, P. Qin, and S. Flach, Anderson localization in generalized discrete-time quantum walks, *Phys. Rev. B* **96**, 144204 (2017).

- [21] S. Derevyanko, Anderson localization of a one-dimensional quantum walker, *Scientific Reports* **8**, 1795 (2018).
- [22] I. Vakulchyk, M. V. Fistul, and S. Flach, Wave packet spreading with disordered nonlinear discrete-time quantum walks, *Phys. Rev. Lett.* **122**, 040501 (2019).
- [23] A. Mallick and S. Flach, Logarithmic expansion of many-body wave packets in random potentials, *Phys. Rev. A* **105**, L020202 (2022).
- [24] X. Guo, J. Sun, W. Cheng, and S. Zhao, Wave packet spreading with periodic, fibonacci quasiperiodic, and random nonlinear discrete-time quantum walks, *Quantum Information Processing* **21**, 393 (2022).
- [25] Y. Omar, N. Paunković, L. Sheridan, and S. Bose, Quantum walk on a line with two entangled particles, *Phys. Rev. A* **74**, 042304 (2006).
- [26] M. Štefanaák, S. M. Barnett, B. Kollár, T. Kiss, and I. Jex, Directional correlations in quantum walks with two particles, *New Journal of Physics* **13**, 033029 (2011).
- [27] A. Ahlbrecht, A. Alberti, D. Meschede, V. B. Scholz, A. H. Werner, and R. F. Werner, Molecular binding in interacting quantum walks, *New Journal of Physics* **14**, 073050 (2012).
- [28] L. Rigovacca and C. Di Franco, Two-walker discrete-time quantum walks on the line with percolation, *Scientific reports* **6**, 22052 (2016).
- [29] M. Malishava, I. Vakulchyk, M. Fistul, and S. Flach, Floquet anderson localization of two interacting discrete time quantum walks, *Phys. Rev. B* **101**, 144201 (2020).
- [30] C. A. Ryan, M. Laforest, J. C. Boileau, and R. Laflamme, Experimental implementation of a discrete-time quantum random walk on an nmr quantum-information processor, *Phys. Rev. A* **72**, 062317 (2005).
- [31] T. Giordani, E. Polino, S. Emiliani, A. Suprano, L. Innocenti, H. Majury, L. Marrucci, M. Paternostro, A. Ferraro, N. Spagnolo, and F. Sciarrino, Experimental engineering of arbitrary qudit states with discrete-time quantum walks, *Phys. Rev. Lett.* **122**, 020503 (2019).
- [32] G. Zhu, L. Xiao, B. Huo, and P. Xue, Photonic discrete-time quantum walks (invited), *Chin. Opt. Lett.* **18**, 052701 (2020).
- [33] M. Gong, S. Wang, C. Zha, M.-C. Chen, H.-L. Huang, Y. Wu, Q. Zhu, Y. Zhao, S. Li, S. Guo, H. Qian, Y. Ye, F. Chen, C. Ying, J. Yu, D. Fan, D. Wu, H. Su, H. Deng, H. Rong, K. Zhang, S. Cao, J. Lin, Y. Xu, L. Sun, C. Guo, N. Li, F. Liang, V. M. Bastidas, K. Nemoto, W. J. Munro, Y.-H. Huo, C.-Y. Lu, C.-Z. Peng, X. Zhu, and J.-W. Pan, Quantum walks on a programmable two-dimensional 62-qubit superconducting processor, *Science* **372**, 948 (2021).
- [34] C. A. Ryan, M. Laforest, J. C. Boileau, and R. Laflamme, Experimental implementation of a discrete-time quantum random walk on an nmr quantum-information processor, *Phys. Rev. A* **72**, 062317 (2005).
- [35] X.-Y. Xu, Q.-Q. Wang, W.-W. Pan, K. Sun, J.-S. Xu, G. Chen, J.-S. Tang, M. Gong, Y.-J. Han, C.-F. Li, and G.-C. Guo, Measuring the winding number in a large-scale chiral quantum walk, *Phys. Rev. Lett.* **120**, 260501 (2018).
- [36] X. Zhan, L. Xiao, Z. Bian, K. Wang, X. Qiu, B. C. Sanders, W. Yi, and P. Xue, Detecting topological invariants in nonunitary discrete-time quantum walks, *Phys. Rev. Lett.* **119**, 130501 (2017).
- [37] B. Tregenna, W. Flanagan, R. Maile, and V. Kendon, Controlling discrete quantum walks: coins and initial states, *New Journal of Physics* **5**, 83 (2003).
- [38] C. M. Chandrashekar, R. Srikanth, and R. Laflamme, Optimizing the discrete time quantum walk using a  $su(2)$  coin, *Phys. Rev. A* **77**, 032326 (2008).
- [39] V. Brosco, L. Pilozzi, R. Fazio, and C. Conti, Non-abelian thouless pumping in a photonic lattice, *Phys. Rev. A* **103**, 063518 (2021).
- [40] L. Pilozzi and V. Brosco, Thouless pumping of light with a twist, *Nature Physics* **18**, 968 (2022).
- [41] R. Citro and M. Aidelsburger, Thouless pumping and topology, *Nature Reviews Physics* **5**, 87 (2023).
- [42] D. J. Thouless, Quantization of particle transport, *Phys. Rev. B* **27**, 6083 (1983).
- [43] F. Wilczek and A. Zee, Appearance of gauge structure in simple dynamical systems, *Phys. Rev. Lett.* **52**, 2111 (1984).
- [44] D. Leykam, A. Andreanov, and S. Flach, Artificial flat band systems: from lattice models to experiments, *Adv. Phys.: X* **3**, 1473052 (2018).
- [45] D. Leykam and S. Flach, Perspective: Photonic flatbands, *APL Photonics* **3**, 070901 (2018).
- [46] R. A. V. Poblete, Photonic flat band dynamics, *Advances in Physics: X* **6**, 1878057 (2021).
- [47] C. Danieli, A. Andreanov, D. Leykam, and S. Flach, Flat band fine-tuning and its photonic applications, *Nanophotonics* **13**, 3925 (2024).
- [48] Y.-K. Sun, X.-L. Zhang, F. Yu, Z.-N. Tian, Q.-D. Chen, and H.-B. Sun, Non-abelian thouless pumping in photonic waveguides, *Nature Physics* **18**, 1080 (2022).
- [49] C. Danieli, V. Brosco, L. Pilozzi, and R. Citro, Non-abelian thouless pumping in a rice-mele ladder, *arXiv2409.20136* (2024).
- [50] V. Brosco, R. Fazio, F. W. J. Hekking, and A. Joye, Non-abelian superconducting pumps, *Phys. Rev. Lett.* **100**, 027002 (2008).
- [51] E. H. Lieb, Two theorems on the hubbard model, *Phys. Rev. Lett.* **62**, 1201 (1989).
- [52] A. Ramachandran, A. Andreanov, and S. Flach, Chiral flat bands: Existence, engineering, and stability, *Phys. Rev. B* **96**, 161104(R) (2017).
- [53] See Supplemental Material at [URL will be inserted by publisher] for additional information.
- [54] M. Santha, Quantum walk based search algorithms, in *Theory and Applications of Models of Computation*, edited by M. Agrawal, D. Du, Z. Duan, and A. Li (Springer Berlin Heidelberg, Berlin, Heidelberg, 2008) pp. 31–46.
- [55] A. M. Childs, Universal computation by quantum walk, *Phys. Rev. Lett.* **102**, 180501 (2009).
- [56] K. Kadian, S. Garhwal, and A. Kumar, Quantum walk and its application domains: A systematic review, *Computer Science Review* **41**, 100419 (2021).
- [57] C. M. Chandrashekar, S. Banerjee, and R. Srikanth, Relationship between quantum walks and relativistic quantum mechanics, *Phys. Rev. A* **81**, 062340 (2010).
- [58] T. Kitagawa, E. Berg, M. Rudner, and E. Demler, Topological characterization of periodically driven quantum systems, *Phys. Rev. B* **82**, 235114 (2010).
- [59] H. Katayama, N. Hatakenaka, and T. Fujii, Floquet-engineered quantum walks, *Scientific Reports* **10**, 17544 (2020).

- [60] T. Kitagawa, M. S. Rudner, E. Berg, and E. Demler, Exploring topological phases with quantum walks, *Phys. Rev. A* **82**, 033429 (2010).
- [61] I. Carneiro, M. Loo, X. Xu, M. Girerd, V. Kendon, and P. L. Knight, Entanglement in coined quantum walks on regular graphs, *New Journal of Physics* **7**, 156 (2005).
- [62] G. Abal, R. Siri, A. Romanelli, and R. Donangelo, Quantum walk on the line: Entanglement and nonlocal initial conditions, *Phys. Rev. A* **73**, 042302 (2006).
- [63] Y. Ide, N. Konno, and T. Machida, Entanglement for discrete-time quantum walks on the line, **11**, 855–866 (2011).
- [64] A. Romanelli, Distribution of chirality in the quantum walk: Markov process and entanglement, *Phys. Rev. A* **81**, 062349 (2010).
- [65] P. Zanardi and M. Rasetti, Holonomic quantum computation, *Physics Letters A* **264**, 94 (1999).
- [66] L.-A. Wu, P. Zanardi, and D. A. Lidar, Holonomic quantum computation in decoherence-free subspaces, *Phys. Rev. Lett.* **95**, 130501 (2005).
- [67] J. Zhang, T. H. Kyaw, S. Filipp, L.-C. Kwek, E. Sjöqvist, and D. Tong, Geometric and holonomic quantum computation, *Physics Reports* **1027**, 1 (2023).
- [68] C. M. Bender and S. A. Orszag, *Advanced mathematical methods for scientists and engineers i: Asymptotic methods and perturbation theory*, Springer Science & Business Media , New York (2013).
- [69] N. Bleistein and R. A. Handelsman, *Asymptotic expansions of integrals*, Ardent Media , New York (1975).

**SUPPLEMENTARY MATERIAL:  
PARITY BREAKING IN THOULESS QUANTUM WALKS**

**PUMPING CYCLES  $\mathcal{C}_{\mathcal{T}}^{++}$ ,  $\mathcal{C}_{\mathcal{T}}^{-+}$ ,  $\mathcal{C}_{\mathcal{T}}^{+-}$  AND  $\mathcal{C}_{\mathcal{T}}^{--}$**

We detail the actions of the pumping cycles  $\mathcal{C}_{\mathcal{T}}^{\xi s}$  upon the symmetric and antisymmetric states  $|p_n\rangle = \frac{|c_n\rangle + |d_n\rangle}{\sqrt{2}}$  and  $|q_n\rangle = \frac{|c_n\rangle - |d_n\rangle}{\sqrt{2}}$ . These cycles  $\mathcal{C}_{\mathcal{T}}^{\xi s}$  are spherical triangles on the hyperplane  $J_c = J_d$  for  $s = +1$  and  $J_c = -J_d$  for  $s = -1$ , and have anti-clockwise orientation for  $\xi = +1$  and clockwise orientation for  $\xi = -1$ . Their corresponding holonomic transformations are

$$W_{\mathcal{C}_{\mathcal{T}}^{\xi s}} = e^{i\xi \frac{k}{2} (\sigma_0 - s\sigma_z)} \quad (9)$$

The four resulting cycles  $\mathcal{C}_{\mathcal{T}}^{++}$ ,  $\mathcal{C}_{\mathcal{T}}^{-+}$ ,  $\mathcal{C}_{\mathcal{T}}^{+-}$  and  $\mathcal{C}_{\mathcal{T}}^{--}$  are shown in Fig. 5(a,d,g,i) and they implement the following operators

$$\mathcal{C}_{\mathcal{T}}^{++} : \sum_n \left[ |p_{n+1}\rangle \langle p_n| + |q_n\rangle \langle q_n| \right] \quad \mathcal{C}_{\mathcal{T}}^{-+} : \sum_n \left[ |p_{n-1}\rangle \langle p_n| + |q_n\rangle \langle q_n| \right] \quad (10)$$

$$\mathcal{C}_{\mathcal{T}}^{+-} : \sum_n \left[ |p_n\rangle \langle p_n| + |q_{n+1}\rangle \langle q_n| \right] \quad \mathcal{C}_{\mathcal{T}}^{--} : \sum_n \left[ |p_n\rangle \langle p_n| + |q_{n-1}\rangle \langle q_n| \right] \quad (11)$$

as explicitly shown in Fig. 5

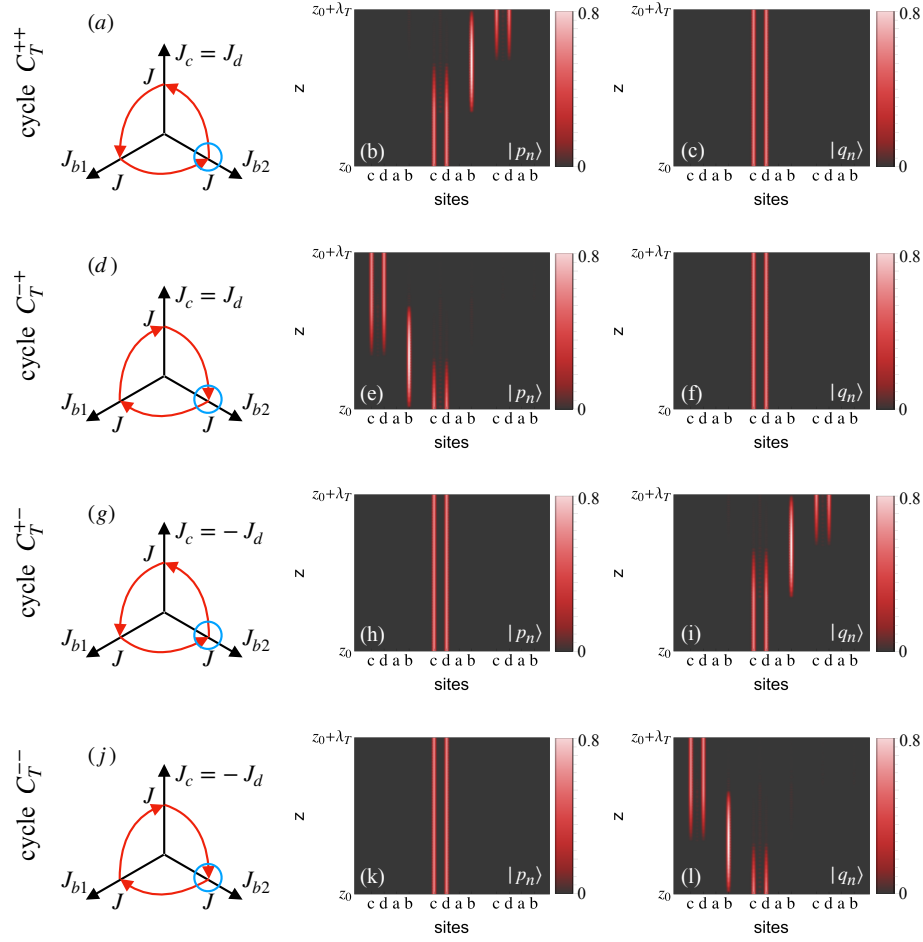


FIG. 5. (a) Sketch of cycle  $\mathcal{C}_{\mathcal{T}}^{++}$ . (b) and (c) Propagation of  $|p_n\rangle$  and  $|q_n\rangle$  respectively over one cycle period. The blue circles indicate the initial point. (d-f) Same as (a-c) for cycle  $\mathcal{C}_{\mathcal{T}}^{-+}$ . (g-i) Same as (a-c) for cycle  $\mathcal{C}_{\mathcal{T}}^{+-}$ . (j-l) Same as (a-c) for cycle  $\mathcal{C}_{\mathcal{T}}^{--}$ .



## DISTRIBUTION

Here we derive an analytical approximation for  $S_n(z_t) = |\psi_n^p(z_t)|^2 + |\psi_n^q(z_t)|^2$  in the long propagation limit following the techniques presented in Refs. [5, 6]. Without loss of generality, we focus on the quantum walk defined via  $\mathcal{C} = \mathcal{C}_T^+ \mathcal{C}_R$ , and for shortness, we indicate the dependence on  $t$  rather than on  $z_t$ .

In vector form, the one time-step advancement from  $t$  to  $t + 1$  reads

$$\begin{aligned} \psi_n(t) &= \begin{pmatrix} \psi_n^p(t) \\ \psi_n^q(t) \end{pmatrix} & \psi_n(t+1) &= \begin{pmatrix} \cos \theta & \sin \theta \\ 0 & 0 \end{pmatrix} \psi_{n-1}(t) + \begin{pmatrix} 0 & 0 \\ -\sin \theta & \cos \theta \end{pmatrix} \psi_n(t) \\ & & &= M_+ \psi_{n-1}(t) + M_0 \psi_n(t) \end{aligned} \quad (12)$$

Switching to k-space,  $\tilde{\psi}_k(t) = \sum_n \psi_n(t) e^{ikn}$ , yields

$$\begin{aligned} \tilde{\psi}_k(t+1) &= \sum_n [M_+ \psi_{n-1}(t) + M_0 \psi_n(t)] e^{ikn} & M_k &= \begin{pmatrix} e^{ik} \cos \theta & e^{ik} \sin \theta \\ -\sin \theta & \cos \theta \end{pmatrix} \\ &= (e^{ik} M_+ + M_0) \sum_n \psi_n(t) e^{ikn} \equiv M_k \tilde{\psi}_k(t) \end{aligned} \quad (13)$$

The matrix  $M_k$  is unitary, and therefore all eigenvalues have absolute value one and the eigenvectors are orthogonal. In this case, the eigenvalues are

$$\lambda_{k,\theta}^{1,2} = e^{i\frac{k}{2}} \left( \cos \theta \cos \frac{k}{2} \pm i \sqrt{1 - \cos^2 \theta \cos^2 \frac{k}{2}} \right) = e^{i\frac{k}{2}} e^{\pm i\Omega_{k,\theta}} \quad (14)$$

where  $\Omega_{k,\theta}$  is an angle with  $\cos \Omega_{k,\theta} = \cos \theta \cos \frac{k}{2}$ . Their corresponding normalized eigenvectors are

$$|w_{k,\theta}^1\rangle \equiv R_{k,\theta} \begin{pmatrix} e^{ik} \sin \theta \\ e^{i\frac{k}{2}} e^{i\Omega_{k,\theta}} - e^{ik} \cos \theta \end{pmatrix} \quad |w_{k,\theta}^2\rangle \equiv T_{k,\theta} \begin{pmatrix} e^{ik} \sin \theta \\ e^{i\frac{k}{2}} e^{-i\Omega_{k,\theta}} - e^{ik} \cos \theta \end{pmatrix} \quad (15)$$

with normalization coefficients defined as  $R_{k,\theta} = \frac{1}{\sqrt{2}} [1 - \cos \theta \cos (\frac{k}{2} - \Omega_{k,\theta})]^{-\frac{1}{2}}$  and  $T_{k,\theta} = \frac{1}{\sqrt{2}} [1 - \cos \theta \cos (\frac{k}{2} + \Omega_{k,\theta})]^{-\frac{1}{2}}$ . We express  $M_k$  through its eigenvalues  $\lambda_{k,\theta}^{1,2}$  (14) and eigenvectors as  $M_k = \lambda_{k,\theta}^1 |w_{k,\theta}^1\rangle \langle w_{k,\theta}^1| + \lambda_{k,\theta}^2 |w_{k,\theta}^2\rangle \langle w_{k,\theta}^2|$ , using the bra-ket notation for the sake of compactness. The dynamics in Eq. (16) can be then recast as

$$\begin{aligned} |\tilde{\psi}_k(t)\rangle &= M_k |\tilde{\psi}_k(t-1)\rangle = M_k^2 |\tilde{\psi}_k(t-2)\rangle = \dots = M_k^t |\tilde{\psi}_k(0)\rangle \\ &= (\lambda_{k,a}^1)^t |w_{k,\theta}^1\rangle \langle w_{k,\theta}^1| \tilde{\psi}_k(0)\rangle + (\lambda_{k,a}^2)^t |w_{k,\theta}^2\rangle \langle w_{k,\theta}^2| \tilde{\psi}_k(0)\rangle \end{aligned} \quad (16)$$

We focus on a single cell initial condition  $|\psi(0)\rangle = \sum_n \delta_{n,0} (a_0 |p_n\rangle + b_0 |q_n\rangle)$  with  $a_0^2 + b_0^2 = 1$ , yielding  $|\tilde{\psi}_k(0)\rangle = (a_0, b_0)$ . By unfolding the projection matrices  $|w_{k,\theta}^1\rangle \langle w_{k,\theta}^1|$  and  $|w_{k,\theta}^2\rangle \langle w_{k,\theta}^2|$ , we obtain:

$$\begin{aligned} |w_{k,\theta}^1\rangle \langle w_{k,\theta}^1| \tilde{\psi}_k(0)\rangle &= R_{k,\theta}^2 \begin{pmatrix} a_0 \sin^2 \theta + b_0 \sin \theta (e^{i\frac{k}{2}} e^{-i\Omega_{k,\theta}} - \cos \theta) \\ a_0 \sin \theta (e^{-i\frac{k}{2}} e^{i\Omega_{k,\theta}} - \cos \theta) + b_0 (R_{k,\theta}^{-2} - 1 + \cos^2 \theta) \end{pmatrix} \\ |w_{k,\theta}^2\rangle \langle w_{k,\theta}^2| \tilde{\psi}_k(0)\rangle &= T_{k,\theta}^2 \begin{pmatrix} a_0 \sin^2 \theta + b_0 \sin \theta (e^{i\frac{k}{2}} e^{i\Omega_{k,\theta}} - \cos \theta) \\ a_0 \sin \theta (e^{-i\frac{k}{2}} e^{-i\Omega_{k,\theta}} - \cos \theta) + b_0 (T_{k,\theta}^{-2} - 1 + \cos^2 \theta) \end{pmatrix} \end{aligned} \quad (17)$$

This leads to the following expressions for the two components of the vector  $|\tilde{\psi}_k(t)\rangle = (\tilde{\psi}_k^p(t), \tilde{\psi}_k^q(t))$

$$\begin{aligned} \tilde{\psi}_k^p(t) &= e^{i\frac{k}{2}t} \left\{ e^{i\Omega_{k,\theta}t} R_{k,\theta}^2 \left[ a_0 \sin^2 \theta + b_0 \sin \theta (e^{i\frac{k}{2}} e^{-i\Omega_{k,\theta}} - \cos \theta) \right] \right. \\ &\quad \left. + e^{-i\Omega_{k,\theta}t} T_{k,\theta}^2 \left[ a_0 \sin^2 \theta + b_0 \sin \theta (e^{i\frac{k}{2}} e^{i\Omega_{k,\theta}} - \cos \theta) \right] \right\} \\ \tilde{\psi}_k^q(t) &= e^{i\frac{k}{2}t} \left\{ e^{i\Omega_{k,\theta}t} R_{k,\theta}^2 \left[ a_0 \sin \theta (e^{-i\frac{k}{2}} e^{i\Omega_{k,\theta}} - \cos \theta) + b_0 (R_{k,\theta}^{-2} - 1 + \cos^2 \theta) \right] \right. \\ &\quad \left. + e^{-i\Omega_{k,\theta}t} T_{k,\theta}^2 \left[ a_0 \sin \theta (e^{-i\frac{k}{2}} e^{-i\Omega_{k,\theta}} - \cos \theta) + b_0 (T_{k,\theta}^{-2} - 1 + \cos^2 \theta) \right] \right\} \end{aligned} \quad (18)$$

By performing the inverse of the Fourier transform  $|\psi_n(t)\rangle = \frac{1}{2\pi} \int_{-\pi}^{\pi} |\tilde{\psi}_k(t)\rangle e^{-ikn} dk$  we obtain the following analytical expression for  $|\psi_n(t)\rangle = (\psi_n^p(t), \psi_n^q(t))$

$$\begin{aligned}\psi_n^p(t) &= \frac{1}{2\pi} \int_{-\pi}^{\pi} e^{i\frac{k}{2}t} \left\{ e^{i\Omega_{k,\theta}t} R_{k,\theta}^2 \left[ a_0 \sin^2 \theta + b_0 \sin \theta (e^{i\frac{k}{2}} e^{-i\Omega_{k,\theta}} - \cos \theta) \right] \right. \\ &\quad \left. + e^{-i\Omega_{k,\theta}t} T_{k,\theta}^2 \left[ a_0 \sin^2 \theta + b_0 \sin \theta (e^{i\frac{k}{2}} e^{i\Omega_{k,\theta}} - \cos \theta) \right] \right\} e^{-ikn} dk \\ \psi_n^q(t) &= \frac{1}{2\pi} \int_{-\pi}^{\pi} e^{i\frac{k}{2}t} \left\{ e^{i\Omega_{k,\theta}t} R_{k,\theta}^2 \left[ a_0 \sin \theta (e^{-i\frac{k}{2}} e^{i\Omega_{k,\theta}} - \cos \theta) + b_0 (R_{k,\theta}^{-2} - 1 + \cos^2 \theta) \right] \right. \\ &\quad \left. + e^{-i\Omega_{k,\theta}t} T_{k,\theta}^2 \left[ a_0 \sin \theta (e^{-i\frac{k}{2}} e^{-i\Omega_{k,\theta}} - \cos \theta) + b_0 (T_{k,\theta}^{-2} - 1 + \cos^2 \theta) \right] \right\} e^{-ikn} dk\end{aligned}\quad (19)$$

To solve the integrals in Eq. (19), let us first observe that  $\Omega_{k,\theta} = \pi - \Omega_{k+2\pi,\theta}$ . Indeed recalling that  $\cos(\pi - x) = -\cos x$  for any  $x$ , it holds that

$$\cos \Omega_{k+2\pi,\theta} = \cos \left( \frac{k+2\pi}{2} \right) \cos \theta = \cos \left( \frac{k}{2} + \pi \right) \cos \theta = -\cos \Omega_{k,\theta} \Rightarrow \Omega_{k+2\pi,\theta} = \pi - \Omega_{k,\theta} \quad (20)$$

This identity implies that  $T_{k,\theta} = R_{k+2\pi,\theta}$  and  $e^{\mp i\Omega_{k,\theta}t} = -e^{\pm i\Omega_{k-2\pi,\theta}t}$ . These identities reduce the integrals to

$$\begin{aligned}\psi_n^p(t) &= \frac{(-1)^t}{\pi} \int_{-\pi}^{\pi} R_{k,\theta}^2 \left[ a_0 \sin^2 \theta + b_0 \sin \theta (e^{i\frac{k}{2}} e^{-i\Omega_{k,\theta}} - \cos \theta) \right] e^{i(\frac{k}{2} + \Omega_{k,\theta})t} e^{-ikn} dk \\ \psi_n^q(t) &= \frac{(-1)^t}{\pi} \int_{-\pi}^{\pi} R_{k,\theta}^2 \left[ a_0 \sin \theta (e^{-i\frac{k}{2}} e^{i\Omega_{k,\theta}} - \cos \theta) + b_0 (R_{k,\theta}^{-2} - 1 + \cos^2 \theta) \right] e^{i(\frac{k}{2} + \Omega_{k,\theta})t} e^{-ikn} dk.\end{aligned}\quad (21)$$

We now recast the exponentials in the above equations by introducing a function  $\phi$  of the parameter  $\alpha = \frac{n}{t}$  obtaining

$$e^{i(\frac{k}{2} + \Omega_{k,\theta})t} e^{-ikn} = e^{i(\frac{k}{2} + \Omega_{k,\theta})t} e^{-ik\alpha t} = e^{i[k(\frac{1}{2} - \alpha) + \Omega_{k,\theta}]t} \equiv e^{i\phi(k,\alpha)t} \quad (22)$$

Therefore, the integrals in Eqs. (21) can be shrunk to

$$\psi_n^p(t) = \int_{-\pi}^{\pi} g_\theta^p(k) e^{i\phi(k,\alpha)t} dk \quad \psi_n^q(t) = \int_{-\pi}^{\pi} g_\theta^q(k) e^{i\phi(k,\alpha)t} dk \quad (23)$$

Integrals of type  $I(t) = \int_a^b f(k) e^{i\phi(k)t} dk$ , alike those in Eq. (23), can be approximated for large  $t$  expanding the phase  $\phi$  to the lowest non-zero order around its stationary point  $c \in ]a, b[$  i.e. setting

$$I(t) = \int_a^b f(k) e^{i\phi(k)t} dk \sim f(c) e^{i\phi(c)t + i\frac{\pi}{2p}} \left[ \frac{p!}{t|\phi^{(p)}(c)|} \right]^{\frac{1}{p}} \frac{\Gamma(1/p)}{p} \quad (24)$$

with  $\phi^{(p)}(c)$  is the first non-zero derivative. More details can be found in Refs. [68, 69]. We use Eq. (24) to approximate the integrals in Eqs. (21,23). The first two derivatives of the function  $\phi$  in Eq. (23) read

$$\begin{aligned}\frac{\partial \phi}{\partial k} &= \frac{1}{2} - \alpha + \partial_k \Omega_{k,\theta} = \frac{1}{2} - \alpha + \frac{1}{2} \frac{\cos \theta \sin \frac{k}{2}}{\sqrt{1 - \cos^2 \theta \cos^2 \frac{k}{2}}} = \frac{1}{2} - \alpha + \frac{1}{2} \frac{\cos \theta \sin \frac{k}{2}}{\sin(\Omega_{k,\theta})} \\ \frac{\partial^2 \phi}{\partial k^2} &= \partial_k^2 \Omega_{k,\theta} = \frac{1}{4} \frac{\cos \theta \sin^2 \theta \cos \frac{k}{2}}{(1 - \cos^2 \theta + \cos^2 \theta \sin^2 \frac{k}{2})^{\frac{3}{2}}} = \frac{1}{4} \frac{\cos(\Omega_{k,\theta}) \sin^2 \theta}{\sin^{\frac{3}{2}}(\Omega_{k,\theta})} = \cot(\Omega_{k,\theta}) [4 - (\partial_k \Omega_{k,\theta})^2]\end{aligned}\quad (25)$$

where we used Eq. (14) to set:  $\sin(\Omega_{k,\theta}) = \sqrt{1 - \cos^2 \theta + \cos^2 \theta \sin^2 \frac{k}{2}}$  and  $\frac{\sin^2 \theta}{\sin^2(\Omega_{k,\theta})} = 1 - 4(\partial_k \Omega_{k,\theta})^2$ . Let us observe that at a given  $\theta$ ,  $\frac{\partial \phi}{\partial k} = 0$  has solutions only for  $\alpha \in ]\frac{1 - \cos \theta}{2}, \frac{1 + \cos \theta}{2}[$  while for  $\alpha$  outside this interval the phase  $\phi(k, \alpha)$  does not have any stationary point. In the latter case the integral in Eq.(24) decreases exponentially as we verify numerically. Recalling  $\alpha = \frac{n}{t}$ , this condition defines the boundaries of the statistical distribution after  $t$  steps as

$$n \in \left[ \frac{t - t \cos \theta}{2}, \frac{t + t \cos \theta}{2} \right]. \quad (26)$$

We now turn our attention to the structure of the distribution in the region inside these boundaries, to estimate it we go back to Eqs.(23) and we calculate  $g_\theta^p, g_\theta^q$  at the stationary point  $\bar{k}$  of  $\phi(k, \alpha)$  which fulfills

$$\sin \frac{\bar{k}}{2} = \tan \theta \frac{2\alpha - 1}{\sqrt{1 - (2\alpha - 1)^2}} \quad (27)$$

This relation yields  $\cos^2 \theta \cos^2 \frac{\bar{k}}{2} = \frac{\cos^2 \theta - (2\alpha - 1)^2}{1 - (2\alpha - 1)^2}$  and, via Eq. (14), leads to

$$\cos(\Omega_{k,\theta}) = \frac{\sqrt{\cos^2 \theta - (2\alpha - 1)^2}}{\sqrt{1 - (2\alpha - 1)^2}} \quad \sin(\Omega_{k,\theta}) = \frac{\sin \theta}{\sqrt{1 - (2\alpha - 1)^2}}. \quad (28)$$

These equations in turn imply

$$e^{i\frac{\bar{k}}{2}} e^{-i\Omega_{k,\theta}} = \frac{1}{2\alpha} \left[ \frac{\cos^2 \theta + 2\alpha - 1}{\cos \theta} - i \tan \theta \sqrt{\cos^2 \theta - (2\alpha - 1)^2} \right] \quad R_{k,\theta} = \frac{\sqrt{2\alpha}}{\sin \theta} \quad (29)$$

where for  $R_{k,\theta}$  we used  $\cos(\frac{\bar{k}}{2} - \Omega_{k,\theta}) = \frac{\cos^2 \theta + 2\alpha - 1}{2\alpha \cos \theta}$ . By substituting Eqs. (28,29) in Eqs. (21,23) we obtain

$$\begin{aligned} g_\theta^p(\bar{k}) &= \frac{(-1)^t}{\pi} \left\{ a_0 2\alpha + b_0 \tan \theta (2\alpha - 1) - i b_0 \frac{\tan \theta}{\sin \theta} \sqrt{\cos^2 \theta - (2\alpha - 1)^2} \right\} \\ g_\theta^q(\bar{k}) &= \frac{(-1)^t}{\pi} \left\{ a_0 \tan \theta (2\alpha - 1) - i a_0 \frac{\tan \theta}{\sin \theta} \sqrt{\cos^2 \theta - (2\alpha - 1)^2} - \frac{b_0}{\sin \theta} (2\alpha - 1) \right\} \end{aligned} \quad (30)$$

From Eq. (23) we get  $|\psi_n^{p,q}(t)|^2 \sim \frac{1}{t} \frac{\pi^2}{|\phi^{(2)}(\bar{k})|} |g_\theta^{p,q}(\bar{k})|^2$  where

$$\frac{1}{|\phi^{(2)}(\bar{k})|} = \frac{\sin \theta}{\sqrt{\cos^2 \theta - (2\alpha - 1)^2} 4\alpha(1 - \alpha)} \quad (31)$$

The absolute values squared of  $g_\theta^p(\bar{k}), g_\theta^q(\bar{k})$  in Eq. (30) are

$$\begin{aligned} |g_\theta^p(\bar{k})|^2 &= \frac{4\alpha}{\pi^2} \{ a_0^2 \alpha - b_0^2 (\alpha - 1) + a_0 b_0 \tan \theta (2\alpha - 1) \} \\ |g_\theta^q(\bar{k})|^2 &= \frac{1}{\pi^2} \{ 4\alpha a_0^2 (1 - \alpha) + b_0 (1 - 2\alpha)^2 (b_0 \csc \theta^2 - 2a_0 \sec \theta) \} \end{aligned} \quad (32)$$

Recalling  $\alpha = \frac{\eta}{t}$ , Eqs. (31,32) yield

$$\begin{aligned} S_n(t) &= |\psi_n^p(t)|^2 + |\psi_n^q(t)|^2 \sim \frac{1}{t} \frac{\pi^2}{|\phi^{(2)}(\bar{k})|} [ |g_\theta^p(\bar{k})|^2 + |g_\theta^q(\bar{k})|^2 ] = \\ &= \frac{1}{t} \frac{\sin \theta \{ 4\alpha(1 - \alpha b_0) + b_0(2\alpha - 1)[(2\alpha - 1)(b_0 \csc \theta^2 - 2a_0 \sec \theta) + 4a_0 \alpha \tan \theta] \}}{\sqrt{\cos^2 \theta - (2\alpha - 1)^2} 4\alpha(1 - \alpha)} \end{aligned} \quad (33)$$

## QUANTUM WALK EQUATIONS AND QUASI-ENERGIES

For quantum walks  $\mathcal{C}_R \mathcal{C}_T^{\xi+}$ , the one time-step advancement from  $t$  to  $t+1$  in vector form reads

$$\begin{pmatrix} \psi_n^p(t+1) \\ \psi_n^q(t+1) \end{pmatrix} = \begin{pmatrix} \cos \theta & \sin \theta \\ 0 & 0 \end{pmatrix} \begin{pmatrix} \psi_{n-\xi}^p(t) \\ \psi_{n-\xi}^q(t) \end{pmatrix} + \begin{pmatrix} 0 & 0 \\ -\sin \theta & \cos \theta \end{pmatrix} \begin{pmatrix} \psi_n^p(t) \\ \psi_n^q(t) \end{pmatrix} \quad (34)$$

Subtract in both sides  $\begin{pmatrix} \psi_n^p(t) \\ \psi_n^q(t) \end{pmatrix}$  and add and subtract in the right hand side  $\begin{pmatrix} \cos \theta & \sin \theta \\ 0 & 0 \end{pmatrix} \begin{pmatrix} \psi_n^p(t) \\ \psi_n^q(t) \end{pmatrix}$ . By introducing the finite difference

$$\partial_t \begin{pmatrix} \psi_n^p(t) \\ \psi_n^q(t) \end{pmatrix} = \begin{pmatrix} \psi_n^p(t+1) \\ \psi_n^q(t+1) \end{pmatrix} - \begin{pmatrix} \psi_n^p(t) \\ \psi_n^q(t) \end{pmatrix} \quad -\xi \partial_n \begin{pmatrix} \psi_n^p(t) \\ \psi_n^q(t) \end{pmatrix} = \begin{pmatrix} \psi_{n-\xi}^p(t) \\ \psi_{n-\xi}^q(t) \end{pmatrix} - \begin{pmatrix} \psi_n^p(t) \\ \psi_n^q(t) \end{pmatrix} \quad (35)$$

Eq. (34) reads

$$\partial_t \begin{pmatrix} \psi_n^p(t) \\ \psi_n^q(t) \end{pmatrix} = -\xi \begin{pmatrix} \cos \theta & \sin \theta \\ 0 & 0 \end{pmatrix} \partial_n \begin{pmatrix} \psi_n^p(t) \\ \psi_n^q(t) \end{pmatrix} + \begin{pmatrix} \cos \theta & \sin \theta \\ -\sin \theta & \cos \theta \end{pmatrix} \begin{pmatrix} \psi_n^p(t) \\ \psi_n^q(t) \end{pmatrix} - \begin{pmatrix} \psi_n^p(t) \\ \psi_n^q(t) \end{pmatrix} \quad (36)$$

Via the Pauli matrixes  $\sigma_i$  and the identity matrix  $\sigma_0$ , Eq. (36) reads

$$\partial_t \begin{pmatrix} \psi_n^p(t) \\ \psi_n^q(t) \end{pmatrix} = -\xi \left[ \cos \theta \frac{\sigma_0 + \sigma_z}{2} + \sin \theta \frac{i\sigma_y + \sigma_x}{2} \right] \partial_n \begin{pmatrix} \psi_n^p(t) \\ \psi_n^q(t) \end{pmatrix} + [(\cos \theta - 1)\mathbb{I} + \sin \theta i\sigma_y] \begin{pmatrix} \psi_n^p(t) \\ \psi_n^q(t) \end{pmatrix} \quad (37)$$

For quantum walks  $\mathcal{C}_{\mathcal{R}}\mathcal{C}_{\mathcal{T}}^{\xi-}$ , the one time-step advancement from  $t$  to  $t+1$  in vector form reads

$$\begin{pmatrix} \psi_n^p(t+1) \\ \psi_n^q(t+1) \end{pmatrix} = \begin{pmatrix} 0 & 0 \\ -\sin \theta & \cos \theta \end{pmatrix} \begin{pmatrix} \psi_{n-\xi}^p(t) \\ \psi_{n-\xi}^q(t) \end{pmatrix} + \begin{pmatrix} \cos \theta & \sin \theta \\ 0 & 0 \end{pmatrix} \begin{pmatrix} \psi_n^p(t) \\ \psi_n^q(t) \end{pmatrix} \quad (38)$$

Alike in the previous case, subtracting in both sides  $\begin{pmatrix} \psi_n^p(t) \\ \psi_n^q(t) \end{pmatrix}$  and add and subtract in the right hand side  $\begin{pmatrix} 0 & 0 \\ -\sin \theta & \cos \theta \end{pmatrix} \begin{pmatrix} \psi_n^p(t) \\ \psi_n^q(t) \end{pmatrix}$ , Eq. (38) reads

$$\partial_t \begin{pmatrix} \psi_n^p(t) \\ \psi_n^q(t) \end{pmatrix} = -\xi \begin{pmatrix} 0 & 0 \\ -\sin \theta & \cos \theta \end{pmatrix} \partial_n \begin{pmatrix} \psi_n^p(t) \\ \psi_n^q(t) \end{pmatrix} + \begin{pmatrix} \cos \theta & \sin \theta \\ -\sin \theta & \cos \theta \end{pmatrix} \begin{pmatrix} \psi_n^p(t) \\ \psi_n^q(t) \end{pmatrix} - \begin{pmatrix} \psi_n^p(t) \\ \psi_n^q(t) \end{pmatrix} \quad (39)$$

Via the Pauli matrixes  $\sigma_i$  and the identity matrix  $\sigma_0$ , Eq. (39) reads

$$\partial_t \begin{pmatrix} \psi_n^p(t) \\ \psi_n^q(t) \end{pmatrix} = -\xi \left[ \cos \theta \frac{\sigma_0 - \sigma_z}{2} + \sin \theta \frac{i\sigma_y - \sigma_x}{2} \right] \partial_n \begin{pmatrix} \psi_n^p(t) \\ \psi_n^q(t) \end{pmatrix} + [(\cos \theta - 1)\mathbb{I} + \sin \theta i\sigma_y] \begin{pmatrix} \psi_n^p(t) \\ \psi_n^q(t) \end{pmatrix} \quad (40)$$

Hence, for quantum walks  $\mathcal{C}_{\mathcal{R}}\mathcal{C}_{\mathcal{T}}^{\xi s}$  the one time-step advancement from  $t$  to  $t+1$  in vector form reads

$$\partial_t \begin{pmatrix} \psi_n^p(t) \\ \psi_n^q(t) \end{pmatrix} = -\xi \left[ \cos \theta \frac{\sigma_0 + s\sigma_z}{2} + \sin \theta \frac{i\sigma_y + s\sigma_x}{2} \right] \partial_n \begin{pmatrix} \psi_n^p(t) \\ \psi_n^q(t) \end{pmatrix} + [(\cos \theta - 1)\mathbb{I} + \sin \theta i\sigma_y] \begin{pmatrix} \psi_n^p(t) \\ \psi_n^q(t) \end{pmatrix} \quad (41)$$

In k-space  $\tilde{\psi}_k(t) = \sum_n \psi_n(t)e^{ikn}$ , the one time-step advancement Eqs. (34,38) relative to a generic oriented quantum walk  $\mathcal{C}_{\mathcal{R}}\mathcal{C}_{\mathcal{T}}^{\xi s}$  reads

$$\tilde{\psi}_k(t+1) = M_k^{\xi s} \tilde{\psi}_k(t) \quad M_k^{\xi s} = \begin{pmatrix} e^{\frac{i}{2}\xi(s+1)k} \cos \theta & e^{\frac{i}{2}\xi(s+1)k} \sin \theta \\ -e^{-\frac{i}{2}\xi(s-1)k} \sin \theta & e^{-\frac{i}{2}\xi(s-1)k} \cos \theta \end{pmatrix} \quad (42)$$

For either  $s = +1$  and  $s = -1$ , their eigenvalues  $\lambda_{k,\theta}^{1,2}$  are

$$\lambda_{k,\theta}^{1,2} = e^{i\xi \frac{k}{2}} \left( \cos \theta \cos \frac{k}{2} \pm i \sqrt{1 - \cos^2 \theta \cos^2 \frac{k}{2}} \right) = e^{i\xi \frac{k}{2}} e^{\pm i\Omega_{k,\theta}} \quad (43)$$

which yield the relation for the quasi-energies  $\lambda_{k,\theta}^{1,2} = e^{iE_{k,\theta}^{1,2}}$

$$\cos E_{k,\theta}^{1,2} = \cos \left[ \frac{k}{2} \pm \Omega_{k,\theta} \right] \quad \Leftrightarrow \quad E_{k,\theta}^{1,2} = \xi \left[ \frac{k}{2} \pm \Omega_{k,\theta} \right] = \xi \left[ \frac{k}{2} \pm \arccos \left( \cos \theta \cos \frac{k}{2} \right) \right] \quad (44)$$

## ENTANGLEMENT ENTROPY: ASYMPTOTIC VALUE

We derive an analytical expression for the asymptotic value of the entropy  $\eta = -\text{Tr}_{\sigma}[\rho_{\sigma} \log_2 \rho_{\sigma}]$  used to estimate the band-position entanglement generated in the quantum walk, following the techniques presented in Ref. [64]. Without loss of generality, we focus on the quantum walk defined via  $\mathcal{C} = \mathcal{C}_{\mathcal{T}}^{\pm} \mathcal{C}_{\mathcal{R}}$ , and for shortness, we indicate the dependence on  $t$  rather than on  $z_t$ .

The reduced density matrix  $\rho_\sigma(t)$  at time-step  $t$  is a  $2 \times 2$  matrix

$$\rho_\sigma(t) = \begin{pmatrix} P_p(t) & Q(t) \\ Q^*(t) & P_q(t) \end{pmatrix} \quad (45)$$

obtained by tracing the total density matrix  $\rho(t) = |\Psi(t)\rangle\langle\Psi(t)|$  over the position index  $n$ , where

$$P_{p(q)}(t) = \sum_n |\psi_n^{p(q)}(t)|^2 \quad Q(t) = \sum_n \psi_n^p(t)\psi_n^{q*}(t) \quad (46)$$

Let us consider the asymptotic reduced density matrix  $\rho_\sigma^\infty = \lim_{t \rightarrow \infty} \rho_\sigma(t) = \begin{pmatrix} P_p^\infty & Q^\infty \\ Q^{\infty*} & P_q^\infty \end{pmatrix}$  and compute the entropy  $\eta_\infty$  via its two eigenvalues  $\mu_1, \mu_2$  as  $\eta_\infty = -\mu_1 \log_2(\mu_1) - \mu_2 \log_2(\mu_2)$ . The off-diagonal term  $Q^\infty$  can be calculated switching to  $k$ -space, as

$$Q^\infty = \lim_{t \rightarrow \infty} Q(t) = \lim_{t \rightarrow \infty} \frac{1}{2\pi} \int_{-\pi}^{\pi} \tilde{\psi}_k^p(t) \tilde{\psi}_k^{q*}(t) dk. \quad (47)$$

This term allows to calculate in the asymptotic limit also the diagonal terms as  $P_p^\infty = \frac{1}{2} + \frac{\text{Re}(Q^\infty)}{\tan \theta}$  and  $P_q^\infty = \frac{1}{2} - \frac{\text{Re}(Q^\infty)}{\tan \theta}$  as demonstrated in Ref. [64]. Via these identities, the eigenvalues  $\mu_1, \mu_2$  of  $\rho_\sigma^\infty$  read

$$\begin{aligned} \mu_{1,2} &= \frac{1}{2} \left[ 1 \pm \sqrt{1 + 4(|Q^\infty|^2 - P_p^\infty P_q^\infty)} \right] \\ &= \frac{1}{2} \left[ 1 \pm \sqrt{1 + 4 \left[ \text{Re}(Q^\infty)^2 + \text{Im}(Q^\infty)^2 - \frac{1}{4} + \frac{\text{Re}(Q^\infty)^2}{\tan^2 \theta} \right]} \right] \end{aligned} \quad (48)$$

We therefore compute explicitly  $Q^\infty$ .

We introduce  $x = a_0 \sin \theta - b_0 \cos \theta$ ,  $y_R = b_0(R_{k,\theta}^{-2} - \sin^2 \theta) - a_0 \sin \theta \cos \theta$ ,  $y_T = b_0(T_{k,\theta}^{-2} - \sin^2 \theta) - a_0 \sin \theta \cos \theta$ ,  $k_- = \frac{k}{2} - \Omega_{k,\theta}$  and  $k_+ = \frac{k}{2} + \Omega_{k,\theta}$  - thus writing  $\tilde{\psi}_k^p(t), \tilde{\psi}_k^q(t)$  in Eq. (18) as

$$\begin{aligned} \tilde{\psi}_k^p(t) &= e^{i\frac{k}{2}t} \{ \alpha_p e^{i\Omega_{k,\theta}t} + \beta_p e^{-i\Omega_{k,\theta}t} \} \\ \tilde{\psi}_k^q(t) &= e^{i\frac{k}{2}t} \{ \alpha_q e^{i\Omega_{k,\theta}t} + \beta_q e^{-i\Omega_{k,\theta}t} \} \end{aligned} \quad (49)$$

where

$$\begin{aligned} \alpha_p &= R_{k,\theta}^2 \sin \theta \left[ a_0 \sin \theta - b_0 \cos \theta + b_0 e^{i(\frac{k}{2} - \Omega_{k,\theta})} \right] = R_{k,\theta}^2 \sin \theta [x + b_0 \cos k_- + ib_0 \sin k_-] \\ \beta_p &= T_{k,\theta}^2 \sin \theta \left[ a_0 \sin \theta - b_0 \cos \theta + b_0 e^{i(\frac{k}{2} + \Omega_{k,\theta})} \right] = T_{k,\theta}^2 \sin \theta [x + b_0 \cos k_+ + ib_0 \sin k_+] \\ \alpha_q &= R_{k,\theta}^2 \sin \theta \left[ a_0 \sin \theta (e^{-i(\frac{k}{2} - \Omega_{k,\theta})} - \cos \theta) + b_0 (R_{k,\theta}^{-2} - \sin^2 \theta) \right] = R_{k,\theta}^2 \sin \theta [y_R + a_0 \sin \theta \cos k_- - ia_0 \sin \theta \sin k_-] \\ \beta_q &= T_{k,\theta}^2 \sin \theta \left[ a_0 \sin \theta (e^{-i(\frac{k}{2} + \Omega_{k,\theta})} - \cos \theta) + b_0 (T_{k,\theta}^{-2} - \sin^2 \theta) \right] = T_{k,\theta}^2 \sin \theta [y_T + a_0 \sin \theta \cos k_+ - ia_0 \sin \theta \sin k_+] \end{aligned} \quad (50)$$

The argument of the integral in Eq. (47) is

$$\tilde{\psi}_k^p(t) \tilde{\psi}_k^{q*}(t) = \alpha_p \alpha_q^* + \beta_p \beta_q^* + \alpha_p \beta_q^* e^{i2\Omega_{k,\theta}t} + \alpha_q^* \beta_p e^{-i2\Omega_{k,\theta}t} \quad (51)$$

However, in the limit  $t \rightarrow \infty$  Eq. (47) reduces to

$$Q^\infty = \frac{1}{2\pi} \int_{-\pi}^{\pi} (\alpha_p \alpha_q^* + \beta_p \beta_q^*) dk \quad (52)$$

Indeed, the integrals  $\int_{-\pi}^{\pi} \alpha_p \beta_q^* e^{i2\Omega_{k,\theta}t} dk$  and  $\int_{-\pi}^{\pi} \alpha_q^* \beta_p e^{-i2\Omega_{k,\theta}t} dk$  involving the third and fourth terms of Eq. (51) are of the form Eq. (23) for  $\alpha = \frac{1}{2}$ . Hence, these integrals vanishes proportionally to  $\frac{1}{t}$  as  $t$  diverges. We split  $Q^\infty$  in

real and imaginary parts as

$$\begin{aligned}\operatorname{Re}(Q^\infty) &= \frac{1}{2\pi} \int_{-\pi}^{\pi} [R_{\alpha_p} R_{\alpha_q} - I_{\alpha_p} I_{\alpha_q} + R_{\beta_p} R_{\beta_q} - I_{\beta_p} I_{\beta_q}] dk \\ \operatorname{Im}(Q^\infty) &= \frac{1}{2\pi} \int_{-\pi}^{\pi} [R_{\alpha_p} I_{\alpha_q} + R_{\alpha_q} I_{\alpha_p} + R_{\beta_p} I_{\beta_q} + R_{\beta_q} I_{\beta_p}] dk\end{aligned}\quad (53)$$

where  $\alpha_p = R_{\alpha_p} + iI_{\alpha_p}$ ,  $\alpha_q^* = R_{\alpha_q} + iI_{\alpha_q}$ ,  $\beta_p = R_{\beta_p} + iI_{\beta_p}$  and  $\beta_q^* = R_{\beta_q} + iI_{\beta_q}$ . Since  $\int_{-\pi}^{\pi} R_{\alpha_p} R_{\alpha_q} - I_{\alpha_p} I_{\alpha_q} dk = \int_{-\pi}^{\pi} R_{\beta_p} R_{\beta_q} - I_{\beta_p} I_{\beta_q} dk$ , the real part  $\operatorname{Re}(Q^\infty)$  reduces to

$$\begin{aligned}\operatorname{Re}(Q^\infty) &= \frac{1}{\pi} \int_{-\pi}^{\pi} [R_{\alpha_p} R_{\alpha_q} - I_{\alpha_p} I_{\alpha_q}] dk \\ &= \frac{1}{\pi} \sin \theta \left\{ \sin \theta [a_0 x - b_0 (b_0 \sin \theta + a_0 \cos \theta)] \int_{-\pi}^{\pi} R_{k,\theta}^4 \cos k_- dk \right. \\ &\quad \left. + \sin \theta [a_0 b_0 - x (b_0 \sin \theta + a_0 \cos \theta)] \int_{-\pi}^{\pi} R_{k,\theta}^4 dk \right. \\ &\quad \left. - 2a_0 b_0 \sin \theta \int_{-\pi}^{\pi} R_{k,\theta}^4 \sin^2 k_- dk + b_0 x \int_{-\pi}^{\pi} R_{k,\theta}^2 dk + b_0^2 \int_{-\pi}^{\pi} R_{k,\theta}^2 \cos k_- dk \right\}\end{aligned}\quad (54)$$

Each integral in Eq. (54) involving  $R_{k,\theta}$ ,  $\cos k_-$  and  $\sin k_-$  respectively are

$$\begin{aligned}\int_{-\pi}^{\pi} R_{k,\theta}^4 \sin^2 k_- dk &= \frac{\pi}{2 \cos^2 \theta} \left( \frac{1}{\sin \theta} - 1 \right) \\ \int_{-\pi}^{\pi} R_{k,\theta}^4 \cos k_- dk &= \frac{\pi}{2 \sin^3 \theta} \left( \frac{1}{\cos \theta \sin \theta} + \frac{\cos \theta}{\sin \theta} - \frac{1}{\cos \theta} \right) \\ \int_{-\pi}^{\pi} R_{k,\theta}^2 \cos k_- dk &= \frac{\pi \cos \theta}{\sin^2 \theta} \\ \int_{-\pi}^{\pi} R_{k,\theta}^4 dk &= \frac{\pi}{\sin^3 \theta} \left( \frac{1}{\sin \theta} - \frac{1}{2} \right) \\ \int_{-\pi}^{\pi} R_{k,\theta}^2 dk &= \frac{\pi}{\sin^2 \theta}\end{aligned}\quad (55)$$

which, given  $a_o = \cos \theta_o$  and  $b_o = \sin \theta_o$ , result in

$$\operatorname{Re}(Q^\infty) = \frac{\sin \theta}{2(1 + \sin \theta)} \cos(\theta - 2\theta_0) \quad (56)$$

The imaginary part  $\operatorname{Im}(Q^\infty)$  in Eq. (53) is instead zero, since  $\int_{-\pi}^{\pi} R_{\alpha_p} I_{\alpha_q} + R_{\alpha_q} I_{\alpha_p} dk = -\int_{-\pi}^{\pi} R_{\beta_p} I_{\beta_q} + R_{\beta_q} I_{\beta_p} dk$ . The eigenvalues  $\mu_1$  and  $\mu_2$  of the asymptotic reduced density matrix  $\rho_\sigma^\infty$  in Eq. (48) reduce to

$$\mu_{1,2} = \frac{1}{2} \left[ 1 \pm \frac{\cos(\theta - 2\theta_0)}{1 + \sin \theta} \right] \quad (57)$$

This yields an analytical formula for the entanglement entropy  $\eta_\infty = -\mu_1 \log_2(\mu_1) - \mu_2 \log_2(\mu_2)$ . In particular, let us observe that for  $\operatorname{Re}(Q^\infty) = 0$  the eigenvalues turn  $\mu_{1,2} = \frac{1}{2}$  which maximize the entropy at  $\eta_\infty = 1$ . Hence, imposing  $\operatorname{Re}(Q^\infty) = 0$  in Eq. (56) yields the condition for maximum entropy

$$\begin{aligned}\operatorname{Re}(Q^\infty) = 0 &\Leftrightarrow \cos(\theta - 2\theta_0) = 0 \\ &\Leftrightarrow \theta = 2\theta_0 \pm \frac{\pi}{2}\end{aligned}\quad (58)$$